

# Reconstruction of simultaneous actuator and sensor faults for the RECONFIGURE benchmark using a sliding mode observer<sup>★</sup>

H. Alwi, L. Chen, C. Edwards

*College of Engineering, Mathematics and Physical Sciences,  
University of Exeter, UK, EX4 4QF.  
(e-mail: h.alwi@exeter.ac.uk, Lejun.Chen@exeter.ac.uk, c.edwards@exeter.ac.uk).*

---

**Abstract:** This paper considers the problem of reconstructing, simultaneously occurring actuator and sensor faults in a nonlinear system. The theory which will be developed in this paper is based on a sliding mode observer formulation, designed around an LPV model approximation of the nonlinear system. It extends previous work which has independently considered actuator and sensor faults reconstruction. Here a single observer structure will be synthesized which can cope with simultaneous actuator and sensor faults. The paper will describe the development of the LPV model, the theory and synthesis of the sliding mode observer, and the results of applying this technique to the RECONFIGURE benchmark problem.

---

## 1. INTRODUCTION

Fault detection and isolation (FDI) and fault tolerant control (FTC) has received a lot of attention in the last few decades with potential applications ranging from industrial processes to aerospace applications. Bearing in mind the wealth of literature, some interesting aerospace application-based FDI/FTC studies can be found in the work carried out during GARTEUR FM-AG16 [Edwards et al. 2010] and ADDSAFE [Goupil and Marcos 2011]. These European projects, were devoted to narrowing the gap between advanced FDI/FTC approaches developed in the academic community and the technical demands of industry. The most recent European study on the potential of FTC for aircraft flight control systems is the EU-FP7 project RECONFIGURE (Reconfiguration of Control in Flight for Integral Global Upset Recovery). The aim of the project is to develop FDI/FTC techniques that facilitate the automated handling of faults and upsets to help alleviate the pilot's tasks during off-nominal/abnormal events, and optimize the aircraft status and flight. This must be performed while maintaining current aircraft safety levels [Pouyou and Goupil 2013b]. In this paper, two RECONFIGURE faults scenarios will be dealt with using one observer design – specifically the detection of faults on the elevator (actuator) and the angle of attack sensor. At the same time, due to the importance of load factor measurement for the existing controller, an additional load factor sensor fault detection problem will also be considered. The FDI scheme proposed in this paper is based on a sliding mode observer designed from a linear parameter varying (LPV) system representation of the plant.

Despite recent developments in sliding mode observers for fault reconstruction e.g. [Tan and Edwards 2003a, Jiang et al. 2004, Alwi et al. 2012, Alwi and Edwards 2013], these schemes only consider actuator and sensor faults individually. The scheme proposed in this paper is different due to its capability to reconstruct both actuator and sensor faults simultaneously using a single observer design. This reduces the design and implementation complexity – especially when dealing with both actuator and sensor faults in the RECONFIGURE project. The work in this

paper also represents one of only a handful of studies which consider LPV based sliding mode designs (see for example [Sivrioglu and Nonami 1998] and more recently [Alwi et al. 2012, Alwi and Edwards 2013, Efimov et al. 2012] for other work which considers LPV based sliding mode controllers/observers). The proposed scheme extends the work in [Tan and Edwards 2003b] (which considers LTI based designs) to LPV systems, therefore ensuring wide coverage of the operating conditions. This paper also describes the development of the LPV model from the RECONFIGURE benchmark which is used for the observer design.

## 2. PROBLEM FORMULATION

Consider an LPV model of the plant represented by

$$\dot{x}_p(t) = A_p(\rho)x_p(t) + B_p(\rho)u(t) + H_p(\rho)f_i(t) + M_p\xi_p(\cdot) \quad (1)$$

$$y_p(t) = C_p(\rho)x_p(t) + D_p(\rho)u(t) + N_p f_o(t) + d_p(t) \quad (2)$$

where  $A_p(\rho) \in \mathbb{R}^{n_n \times n_n}$ ,  $B_p(\rho) \in \mathbb{R}^{n_n \times n_m}$ ,  $C_p(\rho) \in \mathbb{R}^{n_p \times n_n}$ ,  $D_p(\rho) \in \mathbb{R}^{n_p \times n_m}$  and  $H_p(\rho) \in \mathbb{R}^{n_n \times n_h}$  are parameter varying matrices, while  $N_p \in \mathbb{R}^{n_p \times n_q}$  and  $M_p \in \mathbb{R}^{n_n \times n_k}$  are the fixed matrices. In this paper it is assumed that  $(n_h + n_q) < n_p < (n_n + n_q)$  and the parameter  $\rho \in \mathbb{R}^{n_r}$  varies between known extremal values  $\underline{\rho}_i < \rho_i < \bar{\rho}_i$  for  $i = 1, 2, \dots, n_r$ . For the observer design, it is assumed that the matrix  $C_p(\rho)$  has full row rank and the inputs  $u(t)$ , the output measurements  $y_p(t)$  and the varying parameters  $\rho$  are available.

The signals  $f_i(t) \in \mathbb{R}^{n_h}$  and  $f_o(t) \in \mathbb{R}^{n_q}$  represent the (unknown) actuator and sensor faults respectively. Here  $f_i \equiv 0$  and  $f_o \equiv 0$  are associated with fault-free conditions, while either  $f_i \neq 0$  or  $f_o \neq 0$  indicates a fault exists. The signal  $\xi_p(t, y, u) : \mathbb{R}_+ \times \mathbb{R}^{n_p} \times \mathbb{R}^{n_m} \rightarrow \mathbb{R}^{n_k}$  in (1) encapsulates the uncertainty in the system model and captures the plant-model mismatch. It is assumed that  $\xi_p(\cdot)$  is unknown but bounded such that  $\|\xi_p(t, y, u)\| < b$  where  $b$  is a known scalar.

The signal  $d_p(t) \in \mathbb{R}^{n_p}$  in (2) represents a corruption of the true outputs and results in imperfect measurements even in the fault free case where  $f_o \equiv 0$ . A clear distinction is therefore made between sensor measurement corruption

---

<sup>★</sup> This work is supported by EU-FP7 Grant (FP7-AAT-2012-314544): RECONFIGURE

$d_p(t)$  (e.g. ‘disturbance’), and sensor faults  $f_o(t)$  (infrequent but serious effects on the output measurement e.g. biases/drifts/loss of accuracy/freezing etc). This distinction between  $d_p$  and  $f_o$  is made to ensure that  $d_p$  does not cause false alarms. For design purposes, it will be assumed that

$$d_p(s) = G_p(s)\phi(s) \quad (3)$$

where  $G_p(s)$  is a stable transfer function matrix with low pass filter characteristics. The driving signal  $\phi(s)$  is assumed to be unknown but bounded.

### 2.1 Actuator faults

In this paper, it will be assumed that  $H_p(\rho)$  can be factorized as

$$H_p(\rho) = F_p E_p(\rho) \quad (4)$$

Here  $F_p \in \mathbb{R}^{n_n \times n_n}$  is a fixed matrix, while  $E(\rho) \in \mathbb{R}^{n_h \times n_h}$  which is a varying matrix, is assumed to be invertible for all  $\rho$ . The assumption that  $E(\rho)$  is invertible will assist in the fault reconstruction analysis discussed later in the paper.

Using (4), the system in (1) can be rewritten as

$$\dot{x}_p(t) = A_p(\rho)x_p(t) + B_p(\rho)u(t) + F_p \underbrace{E_p(\rho)f_i(t)}_{f_\nu(t,\rho)} + M_p \xi_p(\cdot) \quad (5)$$

where the signal  $f_\nu(t, \rho) : \mathbb{R}_+ \times \mathbb{R}^{n_r} \rightarrow \mathbb{R}^{n_h}$  represents unknown ‘virtual faults’. In the observer design which follows, the ‘virtual faults’  $f_\nu(t, \rho)$  will be estimated initially. Then using the assumption that  $E(\rho)$  is invertible for all  $\rho$ , once  $f_\nu(t, \rho)$  has been estimated, the estimation of the actual fault  $f_i(t)$  can then be obtained.

### 2.2 Sensor faults

From (2), the sensor fault is modelled as an additive perturbation and it is assumed that only  $n_q$  sensors are potentially faulty out of the  $n_p$  output measurements. This is a valid assumption since some sensors may be inherently less reliable or more vulnerable to external effects. Here the columns of  $N_p$  are assumed to be from the standard basis for  $\mathbb{R}^{n_p}$  and that  $N_p$  has full column rank.

Based on this assumption, without loss of generality, the following canonical form can be achieved by permutating the order of the outputs:

$$y_p(t) = \begin{bmatrix} y_{p,1}(t) \\ y_{p,2}(t) \end{bmatrix} \left. \begin{array}{l} \text{fault free} \\ \text{prone to fault} \end{array} \right\} = \underbrace{\begin{bmatrix} C_{p,1} \\ C_{p,2}(\rho) \end{bmatrix}}_{C_p(\rho)} x_p(t) + \underbrace{\begin{bmatrix} D_{p,1}(\rho) \\ D_{p,2}(\rho) \end{bmatrix}}_{D_p(\rho)} u(t) + \underbrace{\begin{bmatrix} 0 \\ I_{n_q} \end{bmatrix}}_{N_p} f_o(t) + \underbrace{\begin{bmatrix} d_{p,1}(t) \\ d_{p,2}(t) \end{bmatrix}}_{d_p} \quad (6)$$

where  $D_{p,2}(\rho) \in \mathbb{R}^{n_q \times n_m}$  and  $C_{p,2}(\rho) \in \mathbb{R}^{n_q \times n_n}$ . In (6), it is assumed that  $C_{p,1} \in \mathbb{R}^{(n_p - n_q) \times n_n}$  has a fixed structure and is independent of  $\rho$ . This assumption is a restriction, but it ensures that an ‘output canonical form’ [Alwi et al. 2011] which will be used later for the observer design, can be achieved.

### 2.3 Augmented System

The first step in designing a consolidated actuator and sensor fault reconstruction formulation is to create the

augmented system. This is achieved by filtering  $y_{p,2}(t)$  (the measurements which are potentially faulty) to create a new state  $z_f(t) \in \mathbb{R}^{n_q}$  given by

$$\dot{z}_f(t) = -A_f z_f(t) + A_f y_{p,2}(t) \quad (7)$$

where (for simplicity)  $A_f \in \mathbb{R}^{n_q \times n_q}$  is a diagonal matrix with positive entries. Substituting for  $y_{p,2}(t)$  from (6) into (7) and augmenting with the systems in (5) yields a new system of order  $(n_n + n_q)$  given by

$$\underbrace{\begin{bmatrix} \dot{x}_p(t) \\ \dot{z}_f(t) \end{bmatrix}}_{\hat{x}(t)} = \underbrace{\begin{bmatrix} A_p(\rho) & 0 \\ A_f C_{p,2}(\rho) & -A_f \end{bmatrix}}_{A(\rho)} \underbrace{\begin{bmatrix} x_p(t) \\ z_f(t) \end{bmatrix}}_{x(t)} + \underbrace{\begin{bmatrix} B_p(\rho) \\ A_f D_{p,2}(\rho) \end{bmatrix}}_{B(\rho)} u(t) + \underbrace{\begin{bmatrix} F_p & 0 \\ 0 & A_f \end{bmatrix}}_F \underbrace{\begin{bmatrix} f_\nu(t, \rho) \\ f_o(t) \end{bmatrix}}_{f(t, \rho)} + \underbrace{\begin{bmatrix} M_p & 0 \\ 0 & A_f \end{bmatrix}}_M \underbrace{\begin{bmatrix} \xi_p(t, y, u) \\ d_{p,2}(t) \end{bmatrix}}_{\xi(t)} \quad (8)$$

The new augmented system ‘output’ is a combination of actual fault free outputs  $y_{p,1}(t)$  with the filtered version of the potentially faulty output  $z_f$ , given by

$$\underbrace{\begin{bmatrix} y_{p,1}(t) \\ z_f(t) \end{bmatrix}}_{y_m(t)} = \underbrace{\begin{bmatrix} C_{p,1} & 0 \\ 0 & I_{n_q} \end{bmatrix}}_C \underbrace{\begin{bmatrix} x_p(t) \\ z_f(t) \end{bmatrix}}_{x(t)} + \underbrace{\begin{bmatrix} D_{p,1}(\rho) \\ 0 \end{bmatrix}}_{D(\rho)} u(t) + \underbrace{\begin{bmatrix} d_{p,1}(t) \\ 0 \end{bmatrix}}_{d(t)} \quad (9)$$

Provided  $\text{rank}(C_{p,1}F_p) = n_h$ , by construction,  $\text{rank}(CF) = \text{rank}(C_{p,1}F_p) + n_q = n_h + n_q$ , and the augmented system in (8) and (9) can be put into the canonical form of [Alwi and Edwards 2013] in the form of an ‘actuator fault reconstruction problem’ [Tan and Edwards 2003a, Alwi and Edwards 2013]. The ‘consolidated fault’ given by  $f(t, \rho)$  in (8), contains both actuator and sensor faults. In the analysis which follows, it will be assumed that  $f(t, \rho)$  in (8) satisfies

$$\|f(t, \rho)\| < a(t, \rho, u) \quad (10)$$

where  $a(t, \rho, u) : \mathbb{R}_+ \times \mathbb{R}^{n_r} \times \mathbb{R}^m \rightarrow \mathbb{R}_+$  is a known function.

## 3. SLIDING MODE OBSERVER

In order to design the sliding mode observer, the augmented system (8)-(9) is first transformed into an output canonical form  $(A(\rho), F, C) \mapsto (\tilde{A}(\rho), \tilde{F}, \tilde{C})$ . This is possible since it is assumed in this paper that  $C_{p,1}$  in (6) is fixed and  $\text{rank}(C_{p,1}F_p) = n_h$ . In these new coordinates  $(\tilde{A}(\rho), \tilde{F}, \tilde{C})$ , the augmented outputs and the fault distribution matrix has the following structure

$$\tilde{C} = [0 \ T] \quad \text{and} \quad \tilde{F} = \begin{bmatrix} 0 \\ 0 \\ F_o \end{bmatrix} \left. \right\} F_2 \quad (11)$$

where  $F_2 \in \mathbb{R}^{n_p \times (n_q + n_h)}$  and  $F_o \in \mathbb{R}^{(n_q + n_h) \times (n_q + n_h)}$  while  $T \in \mathbb{R}^{n_p \times n_p}$  is orthogonal [Alwi and Edwards 2013].

In the new coordinate system associated with  $(\tilde{A}(\rho), \tilde{F}, \tilde{C})$ , the proposed observer for the augmented system (8)-(9) has the structure

$$\dot{\hat{x}}(t) = \tilde{A}(\rho)\hat{x}(t) + \tilde{B}(\rho)u(t) - \tilde{G}_l(\rho)e_y(t) + \tilde{G}_n\nu(t) \quad (12)$$

$$\hat{y}(t) = \tilde{C}\hat{x}(t) + D(\rho)u(t) \quad (13)$$

where  $\tilde{G}_l(\rho)$  and  $\tilde{G}_n \in \mathbb{R}^{(n_n + n_q) \times n_p}$  are the observer gains and  $\hat{x} \in \mathbb{R}^{n_n + n_q}$  is the estimated states. From (9) and (13), the output estimation error

$$e_y(t) = \hat{y}(t) - y_m(t) = \tilde{C}e(t) - d(t) \quad (14)$$

where  $e(t) = \hat{x}(t) - x(t)$ . The term  $\nu(t) \in \mathbb{R}^{n_p}$  in (12) is given by

$$\nu = -\mathcal{K}(t, y, u, \rho) \frac{P_o e_y}{\|P_o e_y\|} \quad (15)$$

and represents the nonlinear injection signal used to induce a sliding motion [Edwards et al. 2000]. Here  $P_o \in \mathbb{R}^{n_p \times n_p}$  is a symmetric positive definite (s.p.d) matrix which satisfies

$$\tilde{A}_{22}^T P_o + P_o \tilde{A}_{22} = -I_{n_p} \quad (16)$$

where the stable matrix  $\tilde{A}_{22} \in \mathbb{R}^{n_p \times n_p}$  in (16) is design freedom which is chosen and fixed. The other design freedom associated with the observer are the gains  $\tilde{G}_l(\rho)$ ,  $\tilde{G}_n$  and the scalar  $\mathcal{K}(t, y, u, \rho)$ . The scalar modulation function  $\mathcal{K}(t, y, u, \rho)$  is chosen so that

$$\mathcal{K}(t, y, u, \rho) > \|CF\|a(t) + \eta_0 \quad (17)$$

where  $\eta_0$  is a positive scalar and  $a(t)$  is the bound on the fault from (10). The state estimation error dynamics obtained from subtracting (8) from (12) are

$$\dot{e}(t) = \tilde{A}(\rho)e(t) - \tilde{G}_l(\rho)e_y(t) + \tilde{G}_n\nu(t) - \tilde{F}f(t) - \tilde{M}\xi(t) \quad (18)$$

The design objective is to select  $\tilde{A}_{22}$ ,  $\tilde{G}_l(\rho)$ ,  $\tilde{G}_n$  and  $\mathcal{K}(t, y, u, \rho)$  in order to force the output estimation error  $e_y(t)$  to zero in finite time, inducing a stable sliding motion on the surface

$$\mathcal{S} = \{e \in \mathbb{R}^{n_n+n_q} : e_y = 0\} \quad (19)$$

During sliding, the signal  $\nu(t)$  can be used to estimate the ‘consolidated fault’ signal  $f(t, \rho)$  using the concept of ‘equivalent output injection’ (i.e. the average value  $\nu(t)$  has to take in order to maintain sliding [Utkin 1992]). As argued in [Alwi and Edwards 2013], the fixed gain  $\tilde{G}_n$  can be chosen as

$$\tilde{G}_n = \begin{bmatrix} -L \\ I_{n_p} \end{bmatrix} \quad (20)$$

where  $L \in \mathbb{R}^{(n_n+n_q-n_p) \times n_p}$  is a design matrix which has the special structure given by

$$L = [L_1 \ 0] \quad (21)$$

with  $L_1 \in \mathbb{R}^{(n_n+n_q-n_p) \times (n_p-n_q)}$ . Once  $L_1$  is determined,  $L$  can be obtained, and therefore the fixed gain  $\tilde{G}_n$  from (20) is determined. Based on  $L$  and the selected matrix  $\tilde{A}_{22}$ , together with sub-matrices extracted from  $A(\rho)$ , the gain  $\tilde{G}_l(\rho)$  from (12) is also determined: for details see [Alwi and Edwards 2013]. The reconstruction signal is given by

$$\hat{f} = W\nu_{eq} \quad (22)$$

where the fixed weighting matrix  $W \in \mathbb{R}^{(n_q+n_h) \times n_p}$  is another design parameter. As proposed in [Alwi and Edwards 2013], the gains  $W$  and  $L_1$  (and thus  $\tilde{G}_n$ ,  $\tilde{G}_l(\rho)$ ) can be synthesized using LMIs, in such a way that the  $\mathcal{L}_2$  gain between the uncertainty  $(\xi, d_p)$  and the fault estimation error  $\hat{f} - f$  is less than a scalar  $\gamma$ . Here for design purposes, it is assumed that  $d(t)$  from (9) emerges from the following exogenous model:

$$\dot{d}(t) = -a_f d(t) + a_f \phi(t) \quad (23)$$

where  $a_f \in \mathbb{R}^+$  and the unknown signal  $\phi(t)$  is assumed to be bounded. In order to minimize the effect of the disturbance  $d(t)$ , the dynamics in (23) is augmented with (8)-(9) and integrated into the LMI optimization framework (as unobservable but detectable dynamics) [Alwi and Edwards 2013]. A ‘tuning knob’ represented by a weighting matrix

$$\Delta = \text{diag}(\delta_1, \delta_2) \quad (24)$$

where  $\delta_1 \in \mathbb{R}^{(n_k+n_q) \times (n_k+n_q)}$  and  $\delta_2 \in \mathbb{R}^{n_p \times n_p}$ , can be used to provide additional design freedom and to introduce a balance between the requirement for the fault estimation to be insensitive to uncertainty in the plant  $\xi(t)$ , and also to be insensitive to imperfect measurements  $\phi(t)$ . Here the weighting matrices  $\delta_1 = \text{diag}(\delta_{1,1} \dots \delta_{1,n_k+n_q})$  and  $\delta_2 = \text{diag}(\delta_{2,1} \dots \delta_{2,n_p})$ .

Using similar arguments to those in [Wei and Verhaegen 2008], it will be assumed that (8) and (9) within the range of admissible  $\rho$ , is represented as a polytopic system  $\mathcal{P}$  with vertices  $\omega_1, \omega_2, \dots, \omega_{n_\omega}$  where  $n_\omega = 2^{n_r}$ . Then using arguments similar to those in [Apkarian et al. 1995], the affine LPV system matrices  $(A(\rho), B(\rho), C, F)$  in (8) and (9) can be replaced by  $(A(\omega_i), B(\omega_i), C, F)$  and the LMIs can be solved for all the vertices of the polytopic system. Further details of the observer synthesis and analysis can be found in [Alwi and Edwards 2013].

### 3.1 fault reconstruction

Reconstruction of the sensor fault  $\hat{f}_o(t)$  can be obtained directly from (22) since  $\hat{f}(t, \rho) = [\hat{f}_\nu(t, \rho) \ \hat{f}_o(t)]^T$  contains a direct estimate of the sensor fault from (8). However for the actuator faults, due to the factorization in (4) and the definition in (5), the fault reconstruction signal from the observer only provides a reconstruction of the ‘virtual’ actuator fault. However, since by assumption  $E_p(\rho)$  is invertible, using the definition in (5), the actual actuator fault can be estimated as

$$\hat{f}_i(t) = E^{-1}(\rho)\hat{f}_\nu(t, \rho) \quad (25)$$

## 4. RECONFIGURE

### 4.1 Reconfigure Benchmark Model

The benchmark model contains detailed actuator and sensor models as well as an existing industrial controller and protection elements [Pouyou and Goupil 2013a]. It has been developed to test the capabilities of new FTC/FDI schemes in various parts of the flight envelope and represents a simplified version of the high fidelity model.

### 4.2 Fault scenarios

In the frame of RECONFIGURE, a set of preliminary fault scenarios are included [Pouyou and Goupil 2013a]. In this paper, two fault scenarios associated with the RECONFIGURE benchmark problem are selected to be dealt with, those are faults on the elevator and angle of attack sensor. Later on, two selected fault scenarios are assumed to occur simultaneously, which increases the design challenge [Edwards et al. 2000, Tan and Edwards 2003b].

### 4.3 Linear affine LPV modelling

In this paper, an *affine* LPV model was built via least squares multivariable polynomial interpolation [Pfiifer and Hecker 2008] from the many different longitudinal LTI models of the RECONFIGURE benchmark.

In fault free, disturbance free and uncertainty free conditions, the affine LPV model is given by

$$\begin{aligned} \dot{x}_p(t) &= A_p(\rho)x_p(t) + B_p(\rho)u(t) \\ y_p(t) &= C_p(\rho)x_p(t) + D_p(\rho)u(t) \end{aligned} \quad (26)$$

Table 1. LPV system inputs

Description	Unit
Left inner elevator ( $\delta_{eil}$ )	deg
Right inner elevator ( $\delta_{eir}$ )	deg
Left outer elevator ( $\delta_{eol}$ )	deg
Right outer elevator ( $\delta_{eor}$ )	deg
Trimmable horizontal stabilizer ( $\delta_{stab}$ )	deg

Table 2. LPV system states

Description	Unit
Pitch rate ( $q$ )	deg/s
Ground speed ( $V_g$ )	m/s
Ground angle of attack ( $\alpha$ )	deg
Pitch angle ( $\theta$ )	deg
Geographical altitude ( $Z_g$ )	m

where,  $\rho \in \mathbb{R}^{n_r}$  represents a set of scheduling parameters and the matrices  $A_p(\rho)$ ,  $B_p(\rho)$ ,  $C_p(\rho)$ , and  $D_p(\rho)$  depend affinely on  $\rho$  as

$$A_p(\rho) = A_{p_0} + \rho_1 A_{p_1} + \dots + \rho_{n_r} A_{p_{n_r}} \quad (27)$$

where,  $A_{p_0}, \dots, A_{p_{n_r}}$  are the LPV system matrices to be obtained. Here, the chosen scheduling parameters are mass  $w$  (tons),  $x$ -position of center of gravity  $cg$  (%/100), Mach number  $M$ , and conventional airspeed  $V_c$  (m/s).

$$\rho = [w \ cg \ V_c \ M] \quad (28)$$

Assume there exists  $k$  grid points throughout the flight envelope at which linearizations are available to be interpolated. Define

$$X = \begin{bmatrix} 1 & 1 & \dots & 1 \\ \rho_{2,1} & \rho_{2,2} & \dots & \rho_{2,k} \\ \vdots & \vdots & \ddots & \vdots \\ \rho_{n_r,1} & \rho_{n_r,2} & \dots & \rho_{n_r,k} \end{bmatrix} \quad (29)$$

where  $X$  is constructed in a linear affine manner.

Suppose the state space system matrix at the  $i$ th grid point is  $S_i$  ( $i = 1, \dots, k$ ). Define

$$S = [S_1 \ S_2 \ \dots \ S_k] \quad (30)$$

then the objective function to calculate  $A_{p_0}, \dots, A_{p_{n_r}}$ , is given by

$$\min_{\mathcal{A}} \|S - AX\|_2 \quad (31)$$

where

$$\mathcal{A} = [A_{p_0} \ A_{p_1} \ \dots \ A_{p_{n_r}}] \quad (32)$$

In order to generate more null elements in the matrix  $\mathcal{A}$ , to reduce the computational load, the mean value of invariant and insignificant elements among the set of LTI models are fixed in  $A_{p_0}$ . In this case, the corresponding elements in the matrices  $A_{p_1} \dots A_{p_{n_r}}$  all become null. The same approach can be used to obtain the other LPV system matrices.

The grid points sampled in the weight/balance domain and  $M/V_c$  domain are shown in Table 4. Combining the weight/balance domain and  $M/V_c$  domain, the resulting affine LPV regions are defined as:

$$w \in [260 \ 405], cg \in [28 \ 36], V_c \in [210 \ 270], M \in [0.4 \ 0.68]$$

The LPV model inputs, states and outputs are shown in Table 1, 2 and 3.

## 5. DESIGN

The RECONFIGURE benchmark problem involves maintaining the normal load factor control law and angle of attack protection in the face of elevator and angle of attack sensor faults/failures. Therefore in this paper only the longitudinal axis will be considered. For the design which

Table 3. LPV system outputs

Description	Unit
Horizontal load factor along aircraft body x-axis ( $n_x$ )	G
Vertical load factor along aircraft body z-axis ( $n_z$ )	G
Vertical speed ( $V_z$ )	ft/s
Pitch rate ( $q$ )	deg/s
Ground speed ( $V_g$ )	m/s
Ground angle of attack ( $\alpha$ )	deg
Pitch angle ( $\theta$ )	deg
Geographical altitude ( $Z_g$ )	m

follows, it will be assumed that the elevator (actuator) as well as load factor and angle of attack sensors are potentially faulty.

The original LPV states are defined in Table 2. To achieve the canonical form required for design, the states have been reordered as

$$x_p = [\alpha \ Z_g \ \theta \ V_g \ q]^T \quad (33)$$

The original input set in Table 1 considers four separate elevators and the stabilizer. Here it is assumed that the elevators are moved in tandem so they have been aggregated to produce a single elevator input signal  $\delta_e$ . The matrix associated with  $B_p(\rho)$  in (1), based on the states in (33), has the form

$$B_p(\rho) = \begin{bmatrix} B_{p,11}(\rho) & B_{p,12}(\rho) \\ 0 & 0 \\ B_{p,41}(\rho) & B_{p,42}(\rho) \\ B_{p,51}(\rho) & B_{p,52}(\rho) \end{bmatrix} \quad (34)$$

Since it is assumed that the elevator is prone to faults, the matrix  $H_p(\rho)$  in (1) is given by the first column of  $B_p(\rho)$  in (34) as

$$H_p(\rho) = [0 \ 0 \ 0 \ 0 \ B_{p,51}(\rho)]^T = \underbrace{\begin{bmatrix} 0_{4 \times 1} \\ 1 \end{bmatrix}}_{F_p} \underbrace{B_{p,51}(\rho)}_{E_p(\rho)} \quad (35)$$

In (34)  $B_{p,11}(\rho) \approx 0$  and  $B_{p,41}(\rho) \approx 0$  due to the fact that the elevator deflection is mainly a pitch moment generator and its contribution to speed  $V_g$  and angle of attack  $\alpha$  is small. This assumption is quite standard in aircraft systems and been considered by many researchers e.g. [Lombaerts 2010]. This allows the  $H_p(\rho)$  in (35) to be factorized into fixed and varying components as given in (4). The effect of ignoring  $B_{p,11}(\rho), B_{p,41}(\rho)$  in (35) will be considered as uncertainty in the  $V_g$  and  $\alpha$  channels and therefore the matrix  $M_p$  in (1) has a structure given by

$$M_p = \begin{bmatrix} 1 & 0 & 0 & 0 & 0 \\ 0 & 0 & 0 & 1 & 0 \end{bmatrix}^T \quad (36)$$

The original outputs are defined in Table 3. For design, the horizontal load factor and vertical speed are not considered as they do not have direct significance for the observer design. To assist in achieving the 'output canonical form' [Alwi and Edwards 2013] the outputs have been reordered to become

$$y_p(t) = \begin{bmatrix} y_{p,1}(t) \\ y_{p,2}(t) \end{bmatrix} = [Z_g \ \theta \ V_g \ q | n_z \ \alpha]^T \quad (37)$$

where  $y_{p,1}(t)$  and  $y_{p,2}(t)$  are associated with the sensors which are fault free and those prone to faults as defined in (6). The matrices  $C_p(\rho)$ ,  $D_p(\rho)$  and  $N_p$  are given by

$$\begin{bmatrix} C_{p,1} \\ C_{p,2}(\rho) \end{bmatrix} = \begin{bmatrix} 0 & 1 & 0 & 0 & 0 \\ 0 & 0 & 1 & 0 & 0 \\ 0 & 0 & 0 & 1 & 0 \\ 0 & 0 & 0 & 0 & 1 \\ C_{p,51}(\rho) & C_{p,52}(\rho) & C_{p,53}(\rho) & C_{p,54}(\rho) & C_{p,55}(\rho) \\ 1 & 0 & 0 & 0 & 0 \end{bmatrix},$$

$$\begin{bmatrix} D_{p,1} \\ D_{p,2}(\rho) \end{bmatrix} = \begin{bmatrix} 0 & 0 \\ 0 & 0 \\ 0 & 0 \\ 0 & 0 \\ D_{p,51}(\rho) & D_{p,51}(\rho) \\ 0 & 0 \end{bmatrix}, N_p = \begin{bmatrix} 0_{4 \times 2} \\ I_2 \end{bmatrix} \quad (38)$$

Note that  $C_{p,1}$  has a fixed structure which fits the assumption made in Section 2.2, while  $D_{p,1} = 0_{4 \times 2}$  (which simplifies the design process).

The variable  $A_f$  which defines the output filter associated with  $y_{p,2}(t) = [n_z \ \alpha]^T$  as shown in (7), has been chosen as  $A_f = I_2$ . The new augmented states and system outputs in the form of (8) and (9) are given by

$$x(t) = [\alpha \ Z_g \ \theta \ V_g \ q | z_{f,1} \ z_{f,2}]^T, y_m(t) = [Z_g \ \theta \ V_g \ q \ z_{f,1} | z_{f,2}]^T \quad (39)$$

where  $z_{f,1}, z_{f,2}$  are the filtered versions of  $n_z$  and  $\alpha$ .

Due to the fixed structure of  $C_{p,1}$ , and the form of  $F_p$  in (38) and (35), plus the fact that  $A_f = I_2$ , the augmented output and fault distribution matrices are given by

$$C = [0_{6 \times 1} \ I_6], F = \begin{bmatrix} 0_{1 \times 3} \\ 0_{3 \times 3} \\ I_3 \end{bmatrix} \quad (40)$$

Note that due to the structure of  $C$  and  $F$  in (40), the augmented system associated with (39) is already in the output canonical form in (11) where  $F_o = I_3$ .

Assuming that the output measurement corruption level is low, the scalar  $a_f$  from (23) is given by  $a_f = 0.01$ . Here it is assumed that the fault estimation is highly affected by the uncertainty in the plant,  $\xi(t)$ , in (8), and less affected by the measurement corruption  $\phi$  in (23). Therefore the weighting matrix in (24) has been chosen as  $\delta_1 = \text{diag}(100, 100, 0, 0)$ ,  $\delta_2 = 0.01 \times \text{diag}(1, 1, 1, 0, 0)$ . It is assumed that the corruption to the filtered state  $z_f(t)$  is negligible and therefore  $d_{p,2}$  in (8) is set as  $d_{p,2} = 0$  and the last two components of  $\delta_1$  and  $\delta_2$  are zero. Solving the LMIs given in detail in [Alwi and Edwards 2013] with the above parameters yields  $L = [35.4237 \ -1.1031 \ 0.0003 \ 0 \ 0 \ 0]$  from (21). The stable design matrix in (16) has been chosen as  $\tilde{A}_{22} = \text{diag}(-10.1, -10.2, -10.3, -10.4, -10.5, -10.6)$ . For implementation purposes, a ‘smooth’ approximation of the discontinuous output injection signal from (15) is used. Specifically  $\nu = -\mathcal{K}(t, y, u, \rho) \frac{P_o e_y}{\|P_o e_y\| + \delta}$  where  $\delta$  is a scalar typically chosen to be small. Here,  $\delta$  has been chosen as  $1 \times 10^{-4}$  and the modulation gain was chosen as  $\mathcal{K}(t, y, u, \rho) = 30$ . For implementation purposes, all the fault reconstruction signals  $\hat{f}$  in (22) are filtered by a simple first order low pass structure with a time constant of 0.2.

## 6. SIMULATION

The results shown in this paper were carried out using the full LPV model in (1) at four of the outer extreme edges of the valid LPV region as well as at one flight condition near the center as shown in Table 4. Note that the existing controller from [Pouyou and Goupil 2013a] is also included in the simulation.

Point	Weight	cg	Vc	Mach	Alt
A	260	28	210	0.40	12500
B	260	36	270	0.51	12500
C	375	28	210	0.54	27500
D	405	36	270	0.68	27500
E	320	28	240	0.53	20000

Table 4. Test points

## 6.1 Results

*Fault free* Figure 1 shows the results for the fault free conditions. Figure 1(a) shows the nominal variation of the states due to the doublet  $n_z$  command at the five different flight conditions. The performance of the observer is shown in terms of the norm of the output error signals  $\|e_y(t)\|$  in Figure 1(c). It can be seen that the difference between the actual and the estimated outputs are close to zero despite the variations in flight conditions, thus indicating that sliding occurs, and the observer provides an accurate estimation of the outputs. Figure 1(c) also shows that no fault is present since the fault reconstruction signals are close to zero. Figure 1(b) shows the nominal elevator and stabilizer deflections. Note that the small stabilizer movement is due to the existing ‘auto trim’ function [Pouyou and Goupil 2013a].

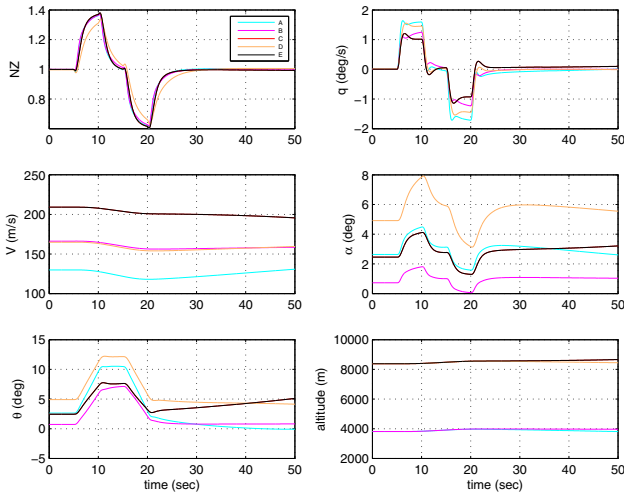
*Simultaneous Actuator and Sensor Faults* Figure 2 shows the results when simultaneous actuator and sensor faults occur at 10 sec, during the  $n_z$  tracking manoeuvre. The elevator and the  $n_z$  and  $\alpha$  sensor faults are modelled as an additive step fault of magnitude of 3 deg, 5 and 0.5 deg respectively. The effect of the additive faults to the elevator,  $n_z$  and  $\alpha$  sensors can be seen in Figure 2(a) and can be compared to the fault free case in Figure 1(a). Note that the  $n_z$  and  $\alpha$  sensor faults only corrupt the measurements which drive the observer. Despite the simultaneous elevator,  $n_z$  and  $\alpha$  sensor faults, sliding still occurs as  $\|e_y(t)\|$  is close to zero as shown in Figure 2(c). Figure 2(c) also shows the reconstructions of the elevator failure and the  $n_z$  and  $\alpha$  sensor faults. Figure 2(c) shows that the reconstructions provide an accurate estimation of the faults and the signals overlap each other. Despite simultaneous actuator and sensor faults and the variation in flight conditions, the reconstruction signal is able to provide accurate estimation of the actual fault.

## 7. CONCLUSION

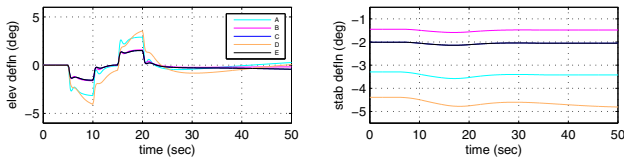
This paper describes the development of a sliding mode observer for simultaneous actuator and sensor fault reconstruction for the RECONFIGURE benchmark problem. The sliding mode observer is designed using a LPV model. Unlike most existing work in the area, the proposed scheme requires only one observer and has the ability to provide simultaneous sensor and actuator fault reconstruction. This paper has presented the theory and development of the LPV based sliding mode observer and also described the development of the LPV model from the RECONFIGURE benchmark. The results show good reconstructions of simultaneous elevator as well as load factor and angle of attack sensor faults at different operating conditions. This highlights the efficacy of the proposed scheme to handle simultaneous sensor and actuator faults over wide variations in flight conditions.

## REFERENCES

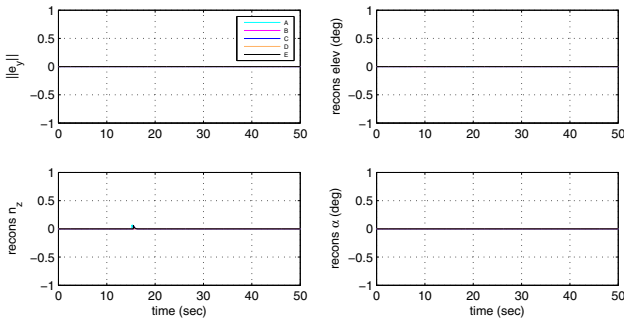
- Alwi, H. and Edwards, C. (2013). Robust fault reconstruction for linear parameter varying systems using sliding mode observers. *International Journal of Robust and Nonlinear Control*, DOI:10.1002/rnc.3009.



(a) States



(b) Surface deflections



(c)  $\|e_y(t)\|$  and fault reconstructions

Fig. 1. Fault free

Alwi, H., Edwards, C., and Marcos, A. (2012). Fault Reconstruction Using a LPV Sliding Mode Observer for a Class of LPV Systems. *Journal of The Franklin Institute*, 349(2), 510–530.

Alwi, H., Edwards, C., and Tan, C.P. (2011). *Fault Detection and Fault-Tolerant Control Using Sliding Modes*. Advances in Industrial Control. Springer-Verlag.

Apkarian, P., Gahinet, P., and Becker, G. (1995). Self-scheduled  $\mathcal{H}_\infty$  control of linear parameter-varying systems: a design example. *Automatica*, 31(9), 1251–1261.

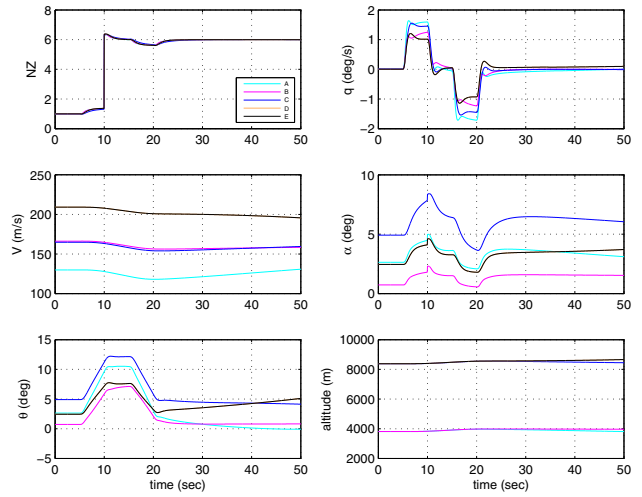
Edwards, C., Lombaerts, T., Smaili, H., and (Eds.) (2010). *Fault Tolerant Flight Control: A Benchmark Challenge*, volume 399. Springer-Verlag: Lecture Notes in Control and Information Sciences.

Edwards, C., Spurgeon, S., and Patton, R. (2000). Sliding mode observers for fault detection. *Automatica*, 36, 541–553.

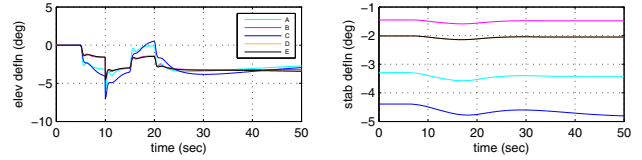
Efimov, D., Fridman, L., Raissi, T., Zolghadri, A., and Seydou, R. (2012). Interval estimation for LPV systems applying high order sliding mode techniques. *Automatica*, 48(9), 2365–2371.

Goupil, P. and Marcos, A. (2011). Advanced Diagnosis for Sustainable Flight Guidance and Control: The European ADDSAFE Project. In *SAE AeroTech Congress & Exhibition*, doi:10.4271/2011-01-2804.

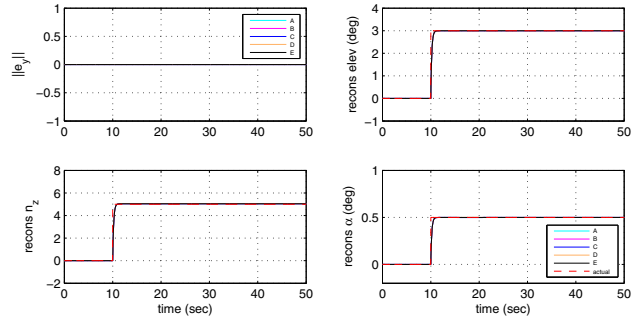
Jiang, B., Staroswiecki, M., and Cocquempot, V. (2004). Fault estimation in nonlinear uncertain systems using robust sliding-mode observers. *IEE Proceedings: Control Theory & Applications*, 151, 29–37.



(a) States



(b) Surface deflections



(c)  $\|e_y(t)\|$  and fault reconstructions

Fig. 2. Simultaneous elevator,  $n_z$  sensor and  $\alpha$  sensor fault

Lombaerts, T. (2010). *Fault Tolerant Flight Control: A Physical Model Approach*. Ph.D. thesis, Delft University of Technology.

Pfifer, H. and Hecker, S. (2008). Generation of optimal linear parametric models for LFT-based robust stability analysis and control design. In *Proceedings of the 47th IEEE Conference on Decision and Control, CDC*, 3866–3871.

Pouyou, G. and Goupil, P. (2013a). Benchmark definition and user manual. RECONFIGURE Technical Note D1.1.3, AIRBUS.

Pouyou, G. and Goupil, P. (2013b). Benchmark scenario definition. RECONFIGURE Technical Note D1.1.2, AIRBUS.

Sivrioglu, S. and Nonami, K. (1998). Sliding mode control with time-varying hyperplane for AMB systems. *IEEE/ASME Transactions On Mechatronics*, 3(1), 51–59.

Tan, C.P. and Edwards, C. (2003a). Sliding mode observers for robust detection and reconstruction of actuator and sensor faults. *International Journal of Robust and Nonlinear Control*, 13, 443–463.

Tan, C. and Edwards, C. (2003b). Sliding mode observers for reconstruction of simultaneous actuator and sensor faults. In *Proceedings of the Conference on Decision and Control, CDC '03, Hawaii*, 1455–1460.

Utkin, V.I. (1992). *Sliding Modes in Control Optimization*. Springer-Verlag, Berlin.

Wei, X. and Verhaegen, M. (2008). Mixed  $\mathcal{H}_2/\mathcal{H}_\infty$  fault detection observer design for LPV systems. In *IEEE Conference on Decision and Control*, 1073–1078.